Investigation of the influence of oil injection upon the screw compressor working process*

N. Stošić, Lj. Milutinović, K. Hanjalić and A. Kovačević
Mechanical Engineering Faculty, University of Sarajevo, 71000 Sarajevo, Yugoslavia
Received 13 March 1991; revised 28 July 1991

Some results of mathematical modelling and experimental investigation of the influence of oil injection upon the screw compressor working process are presented. Several parameters that characterize oil injection were varied over ranges that were initially determined from a computer model. These include: oil flowrate, inlet temperature, droplet atomization, positions in the casing at which the oil was injected, oil jet speed and angle, and time of oil retention in the working volume. The compressor performances were evaluated from measurements of all important bulk parameters: delivery rate, power consumption, power utilization efficiency, specific power, as well as the instantaneous pressure and temperature at several positions along the working volume, from which the indicator diagram was worked out. In addition to the information about the influence of each oil parameter upon the compressor performances, the collected data served to verify and complement the mathematical model of the influence of oil upon the screw compressor working process developed earlier, which has subsequently been employed for computer-aided design of two different screw-compressor oil systems. The experimental results and the application of the computer simulation helped in modifying the oil injection system, which resulted in a saving in compressor energy consumption up to 7%.
(Keywords: screw compressor; oil injection; computer-aided design)

Étude de l'influence de l'injection d'huile sur le fonctionnement d'un compresseur à vis

On présente quelques résultats de la modélisation mathématique et de recherches expérimentales sur l'influence de l'injection d'huile sur le fonctionnement d'un compresseur à vis. Plusieurs paramètres caractérisant l'injection d'huile ont été modifiés à l'intérieur de plages initialement déterminées avec un modèle informatique. Ces paramètres sont les suivants: débit masse de l'huile, température d'entrée, degré d'atomisation des gouttelettes, point d'injection d'huile dans le carter, vitesse et angle du jet d'huile, et durée et la rétention d'huile dans le volume de travail. On a évalué les performances du compresseur en mesurant l'ensemble de tous les paramètres importants: débit, consommation d'électricité, rentabilité énergétique, puissance spécifique, ainsi que pression instantanée et température en plusieurs localisations le long du volume de travail. Ces paramètres ont permis de tracer le diagramme indicatif. Les données obtenues ont servi, non seulement à recueillir des informations sur l'influence de chacun des paramètres d'huile sur les performances du compresseur, mais aussi à vérifier et à améliorer le modèle mathématique de l'influence de l'huile sur le fonctionnement du compresseur à vis, développé antérieurement et que l'on a ensuite utilisé pour la conception assistée par ordinateur de deux systèmes différents d'huile pour les compresseurs à vis. Les résultats expérimentaux et l'application de la simulation informatique ont aidé à modifier le système d'injection d'huile, ce qui a permis de réaliser une économie de la consommation d'énergie du compresseur de l'ordre de 7%.
(Mots clés: compresseur à vis; injection d'huile; conception assistée par ordinateur)

Among a variety of displacement compressor designs, screw compressors, with their compactness, robustness, long durability, excellent performance over a wide range of operating conditions and other advantages, are used increasingly for the supply of compressed gases in various branches of process and other industries. As a rotating machine of a relatively simple design (without any oscillating elements) it can develop a high rotational speed and consequently a high power and efficiency per unit weight, as well as a wide range of operating pressure and delivery. However, the performance of a screw compressor is very sensitive to a number of design parameters governing the thermodynamic and flow process[2,16,17]. A particularly strong influence is exerted by the oil injection, which, in addition to the lubricating, provides better sealing and gas cooling.

The classic approach to the design of new machines like screw compressors rested in the past on the ideas of shrewd inventors and on subsequent systematic experimental testing and evaluation of effects of all relevant factors upon the working process and energy conversion efficiency. Nowadays a great deal of this lengthy and tedious work (including the verification of original ideas) can be substituted by mathematical modelling and computer simulation of a process as a whole, or of individual phenomena that constitute such a process. The solution of modelled equations can yield reliable predictions of compressor performances for the prescribed input

*This paper was first presented in condensed form at the Compressor Technology Conference held at Purdue University, 17–20 July 1990.

0140–7007/92/010016–15

variables, enabling even an easy and fast arrival at optimum combinations of design parameters and working conditions. Mathematical modelling has become the basic ingredient of the computer-aided design (CAD) approach, which now serves as a tool for compressor design and optimization.

A consistent mathematical model employs the exact kinematic relationship in differential form that describes the instantaneous operating volume and its changes with time or rotation angle, as well as the equations of conservation of mass and energy for the control volume adopted[3,6,10,26]. Major, still unresolved, differences among various models appear in the approach to the modelling of various accompanying phenomena, which cannot easily be represented by general analytical formulations, such as fluid leakage, oil injection, heat transfer between gas on one side and screws and compressor housing on the other, and others, which influence to a large extent the final performances of a real compressor. Because of these uncertainties, mathematical modelling and computer simulation have their limitations and the final answers have to be obtained eventually on a test bench in a laboratory. Of course, the task is now easier since computer optimization has reduced the uncertainties and the range of possible variation of most parameters in question. This approach has been adopted in our work on the development of a new family of screw compressors. The mathematical model, developed and verified through a detailed laboratory test of a selected screw compressor, served as a basis for deciding on most major parameters. The final optimization was achieved by careful and systematic experimental investigations of all factors that could not be decided upon with reliable certainty by computer modelling.

One of the most important problems, which requires careful investigation, is the influence of oil injected into the working volume of most types of screw compressors for the purposes of sealing, cooling and lubrication. As is well known, injected oil considerably affects thermodynamic processes in the compressor. Better sealing means less gas leakage and the improvement of the compression and delivery rates. In addition, an increase in the mass rate of the working fluid due to oil injection lowers the compression temperatures, allowing higher compression rates[4,9]. Several parameters that play an important role in this process have to be optimized by the designer in order to achieve the best effects and the analysis of the influences of these parameters has been the subject of our investigation. These are: the size of oil droplet, oil-inlet temperature, position and size of oil-inlet port, velocity of the oil jet and oil viscosity. This paper focuses on the experimental investigation of the influence of oil injection upon the process in a screw compressor. A detailed study of the same problem was made by computer modelling, as reported earlier[23], and the present work represents both the experimental verification of the model as well as the complementary research aimed at collecting experimentally those data that could not be obtained by the simulation model.

The experiments were made on two engine prototypes of the major Yugoslav compressor manufacturer Energoinvest-Trudbenik. A detailed account is presented of the experience gained in the selection of measurement methods, preparation of instruments, acquisition and processing of the data measured, with a particular emphasis on the mounting and connection of the high-resolution pressure gauges within the engines tested[12]. The investigation was focused on the analysis and optimization of three factors that contribute a great deal to the optimum effect of oil injection upon the screw compressor process: conditions for appropriate atomization of the oil; increase of the oil droplets' retention time in a working space; determination of the optimum oil:gas ratio to produce a minimum compressor specific power. Each of these aspects will be elaborated in detail.

Mathematical modelling

Model of the screw compressor working process

A generalized approach has been applied, which implies the computation of screw compressor thermodynamic processes by the numerical solution of the set of differential equations for energy, and continuity with appropriate initial and boundary conditions[3,6,26]. For a screw compressor, equations have a simple form and in our model they were derived on the basis of the following assumptions (which ensure a sufficient degree of generality for a wider application):

(a) Working fluid, encountered in the model, could be any gas of known equation of state and relations for internal thermal energy and enthalpy, i.e. any ideal or real gas or gas–oil mixture;
(b) Heat transfer between gas and compressor screws or its casing was incorporated into the model;
(c) Gas or gas–oil mixture inflow or outflow through the compressor suction or discharge openings was assumed isentropic;
(d) Gas or gas–oil mixture leakages, which can occur in any stage of the process through the clearance between the moving and stationary parts of the engine, were assumed isenthalpic;
(e) Oil was allowed to be injected during all of the compressor process stages (suction, compression or discharge) and it affected all of them.

The temperature of the oil droplets and the gas during all of the processes could be different according to the gas–oil heat transfer conditions. The approach adopted differs from the common one in choosing the internal energy as a dependent variable instead of pressure or enthalpy, which was the usual practice before.

The extension of the model application presented here concerns the investigation of the influence of oil on the screw compressor process. The injection of lubricating oil has a strong effect upon the total energy interchange between the fluid and the engine[20]. The oil temperatures, oil:gas mass ratios, oil droplet sizes and locations of oil-injection ports were varied over a wide range to obtain the necessary information about the influence of oil on the working process of the compressor. The history of pressure and temperatures of gas and oil during the compressor cycle and the volumetric and power utilization efficiencies, as well as specific powers, were compared for different input data variations.

The conservation equation for the internal energy in terms of the angle of rotation α for the control volume (compressor working volume) can be written as

$$\frac{\mathrm{d}U}{\mathrm{d}\alpha} = i_{\mathrm{in}}\left(\frac{\mathrm{d}m}{\mathrm{d}\alpha}\right)_{\mathrm{in}} - i_{\mathrm{out}}\left(\frac{\mathrm{d}m}{\mathrm{d}\alpha}\right)_{\mathrm{out}} + \frac{\mathrm{d}Q}{\mathrm{d}\alpha} - \frac{\mathrm{d}W}{\mathrm{d}\alpha} \quad (1)$$

where i is fluid enthalpy, Q and W are heat and work, respectively, exchanged between the system and its surroundings through the control surface, and the subscripts 'in' and 'out' denote the control volume inlet and outlet. If the working fluid is a mixture of gas and oil droplets, the terms of the equation can be expressed in the form

$$i_{in}\left(\frac{dm}{d\alpha}\right)_{in} = (i_g)_{in}\left(\frac{dm_g}{d\alpha}\right)_{in} + (i_o)_{in}\left(\frac{dm_o}{d\alpha}\right)_{in}$$

$$i_{out}\left(\frac{dm}{d\alpha}\right)_{out} = (i_{mix})_{out}\left(\frac{dm_{mix}}{d\alpha}\right)_{out}$$

$$\frac{dQ}{d\alpha} = \frac{Ah}{\omega}(T_s - T) \qquad \frac{dW}{d\varphi} = -p\frac{dV}{d\alpha}$$

where: i denotes enthalpy per unit mass; p, pressure; T, temperature; V, compressor volume; A, heat transfer area; ω, rotating speed; h, heat transfer coefficient with indices meaning: gas, g; oil, o; mixture, mix; and surface, s.

Together with the continuity equation

$$\frac{dm}{d\alpha} = \frac{\rho w A_f}{\omega} \tag{2}$$

where A_f denotes the effective flow area changing its geometry and flow conditions in time, w denotes fluid velocity and ρ, fluid density, Equations (1) and (2) form a system of differential equations describing the screw-compressor thermodynamic process. The right-hand side of the energy equation consists of the following terms, which have been appropriately modelled:

1. The energy gain due to the gas inflow into the working volume is represented by the gas enthalpy and change of its mass ($dm/d\alpha$). During suction gas enters the working volume bringing gas enthalpy that prevails in the suction chamber. However, during the time when the suction opening is closed, some gas leaks through clearances filling the working space of the compressor. The mass of this gas, as well as its enthalpy, is determined on the basis of the gas-leakage continuity and energy equations, which describe isoenthalpy flow with friction. The shape and dimensions of gaps, gas parameters before and after the gap, flow length, friction and local inflow and outflow losses due to the sudden flow area changes are accounted for.
2. The energy loss due to gas outflow from the working volume is determined by its mass and outgoing gas enthalpy. During the compression this is the gas that leaks through the clearance from the working volume into the surrounding space.
3. Mechanical work brought to the gas during the working process is positive if the volume of the working space is decreased. The gradient $dV/d\alpha$ is obtained from the kinematic relations of a screw rotor.
4. The effect of the heat exchange between the fluid and screw rotors and casing due to the different temperatures of the gas and the rotors and casing surfaces is accounted for through the simple cooling law with heat transfer coefficient determined on the basis of the expression $Nu = 0.023\ Re^{0.8}$, which is supposed to hold reasonably well for the conditions considered. The characteristic length and velocity in the Reynolds number are obtained from the compressor geometry.

If the oil is injected into the compressor volume, the oil mass and its enthalpy should be accounted for.

In order to enhance oil cooling efficiency (gas–oil heat transfer) the surface area of the oil droplet should be as large as possible for the same quantity of oil defined by lubricating requirements. To this end, the oil was atomized in small droplets by generating an oil spray in which the distribution of the droplets sizes (represented by droplet radius r) is defined by the following differential equation:

$$\frac{dn}{dr} = a\, r^p \exp(-br^q) \tag{3}$$

where a, b, p and q are distribution coefficients depending on oil:gas flow and velocity ratios. The atomization of oil is achieved by a simple high-pressure injection of an oil jet in the spacing between the main and gate screw rotors. During the injection of oil, a period of oil-jet destruction and a period of oil-spray formation can be identified. These time periods are lowered with increasing gas density, oil:gas relative velocity and nozzle diameter. The mean Sauter diameter, for a general distribution of droplet sizes, is defined by

$$r = 0.0183\left(\frac{\rho_o \sigma_o}{w}\right)\left(1 + \frac{m}{m_o}\right)^{0.7} \tag{4}$$

Oil droplets are supposed to be spherical with known mean Sauter diameter. Heat transfer between the gas and oil droplets is defined by the simple cooling law $Q = hA(T - T_o)\Delta\alpha/\omega$, where h stands for the heat transfer coefficient, A is the average droplet surface area and T and T_o are gas and oil temperatures. The heat transferred must also satisfy another equation, $Q = m_o c_o(T_o - T_{ob})$, where m_o is the oil mass rate, c_o is the specific heat of oil, and T_{ob} is the oil temperature in the previous time step.

The heat transfer coefficient h at the spherical droplet surface for Stokes flow is obtained from the expression

$$Nu = 2 + 0.6\ Re^{0.6} Pr^{0.33} \tag{5}$$

where the oil velocity in Reynolds number is determined from the oil mass rate injected through the oil orifice. In order to define Re and Nu numbers the mean droplet diameter d was used as suggested by Sauter. A range of droplet diameters from 0 to 1 mm was covered in the mathematical model to examine the influence of droplet size upon the working process of a screw compressor.

The oil temperature is obtained directly from heat transferred from gas to oil as:

$$T_o = \frac{T + kT_{ob}}{(1 + k)} \tag{6}$$

where $k = m_o c_o \omega / hA\Delta\alpha = r\rho_o c_o / 3h\Delta\alpha$ is the time constant, r is the oil droplet radius and ρ_o is the oil density.

In the continuity Equation (2), the density ρ is obtained from the known mass and volume V as $\rho = m/V$, and the suction and discharge-opening cross sectional surface area. These areas, as well as the area of the gap clearance betwen the mobile parts of the compressor, can be calculated from the known compressor kinematics, and the flowrate through these openings from the energy equation and the rate of change of momentum depending on the character of the flow. In our model, the flow through the suction and discharge

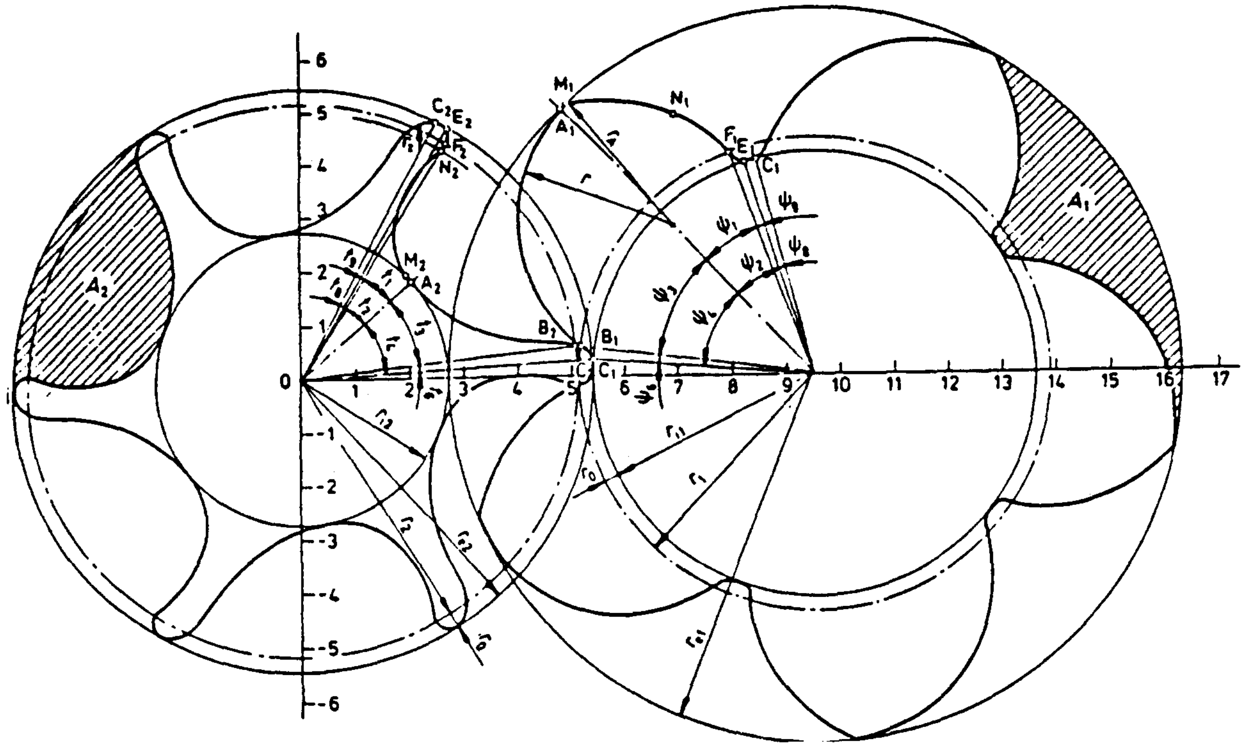

Figure 1 Screw compressor configuration: basic dimensions and notation
Figure 1 *Configuration du compresseur à vis: dimensions fondamentales et annotation*

opening is considered as adiabatic, and gas leakage through the clearances is considered as isenthalpic, for which the corresponding differential relations exist.

As a supplement to the basic differential equations of the compressor thermodynamic process, several constitutive algebraic relations are to be added. These include the equation of state. If the gas can be treated as ideal, the internal thermal energy of the gas–oil mixture is given by:

$$U = m_g u_g + m_o u_o = \frac{mRT}{(\kappa - 1)} + m_o c_o T_o = \frac{pV}{(\kappa - 1)} + m_o c_o T_o \qquad (7)$$

where R denotes the gas constant. Hence, from Equation (7) either the pressure or temperature of the fluid in the compressor working space can be explicitly calculated with the help of the equation for gas–oil heat transfer, which gives the gas temperature

$$T = (\kappa - 1)\frac{(1 + k)U - m_o c_o T_o}{(1 + k)mR + m_o c_o} \qquad (8)$$

It is obvious that for $k = 0$ (high heat transfer coefficients or small oil droplet size) the oil temperature approaches the gas temperature. The situation is rather more complex if the equation of state of a real gas is considered, $p = f_1(T,V)$, for example in references 15 and 21, which with the equation for internal energy of real gas, $u = f_2(T)$ and with the equation for internal energy (1) form a system of equations. After the internal thermal energy U and mass of the gas in screw compressor working volume are determined, the resulting system of algebraic equations is usually decoupled, and can be conveniently solved by a numerical method.

The modelled differential equations are solved by means of a Runge–Kutta fourth-order procedure. Since the initial conditions are arbitrarily selected, the convergence of the solution is obtained after the difference between the two consecutive compressor cycles showed a sufficiently small value prescribed in advance.

Discussion

The investigation of the influence of oil injection upon the screw-compressor thermodynamic cycle was made through the analysis of the individual effects of the following oil parameters: the size of oil droplet; oil inlet temperature; position of oil inlet port and the oil viscosity. The compressor considered had the following characteristic dimensions: distance between the rotor pairs a, 75 mm; helix angle, 45°; designed gap clearance, 0.09 mm (*Figure 1*). The compression process starts at 0° and finishes at 298° of the male-rotor rotation angle. More information can be found in reference 25. A view of the compressor considered is given in *Figure 2*.

In order to cover all the expected sizes of the droplets, a wide range of diameters from 0 to 1 mm was considered. The oil inlet temperature varied from 293 to 373 K, while the oil:gas mass ratio varied from 0 (dry gas) to 8. A range of position angles of the oil inlet port from 0 to 270° was also considered. In addition, five types of oil, each of different viscosity, denoted simply by labels 1–5, were tested. A different oil type produces a different clearance gap, which is selected as an input parameter. Volumetric efficiency (delivery flowrate normalized by the theoretical delivery), power efficiency (isothermal power normalized by indicated one) and specific power (indicated power normalized by flowrate) were selected as output parameters. All considered input values, together with volumetric and power efficiency and specific power, are listed in *Tables 1* and *2*.

Figures 3–6 show the calculated temperatures of gas

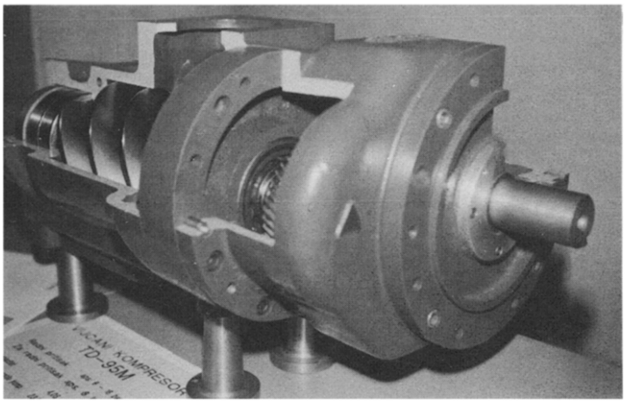

Figure 2 A view of the Trudbenik screw compressor
Figure 2 *Coupe du compresseur à vis "Trudbenik"*

Table 1 Input conditions
Tableau 1 *Données d'entrée*

Speed of rotation, ω	4222 m s^{-1}
Suction ambient pressure, p_0	1 bar
Discharge pressure, p	6 bar
Compressing gas constant, R	287 J kg^{-1} K^{-1}
Tip speed, w	30 m s^{-1}
Suction temperature, T_0	288 K
Rotor/housing temperature, T_s	333 K
Specific heat ratio, κ	1.4

and oil as a function of the rotational angle during a compressor cycle for different droplet sizes. It is clearly visible that the oil and gas temperatures have the same value for a wide range of droplet sizes, almost up to 100 μm, and even for quite large droplets of 0.5 mm, the gas–oil temperature difference is still less than 30°C. These results confirm the assumption that the value of the oil temperature in screw compressors cannot be considered to be the same as the gas temperature, since it may be different if oil droplets are allowed to reach the housing surface due to inertial forces and to form an oil film, which would cause different heat transfer conditions.

In *Figures 7–10* the gas and oil temperatures are plotted over the rotational angle for different oil-inlet temperatures, oil-inlet positions, oil–gas mass flow ratio and for different oil types. It can be seen that the oil temperature has a strong influence on the gas exit temperature. In fact, it affects the gas temperature over the whole cycle, thereby influencing the compressor power efficiency, but at the same time exerting only a minor influence on the volumetric efficiency. The opposite situation prevails if different oil types are considered, when both the power and volumetric efficiencies are considerably affected, but with only a slight influence on the gas outlet temperature. For low oil:gas mass ratios the effects upon the compressor process are more visible than for higher mass ratios, which indicates a possibility for an optimization of the oil temperature and oil:gas mass ratio, especially if other equipment, like oil removers and oil coolers, are considered.

The position of the oil-inlet port has a strong influence on the gas temperature during the cycle, but it has no influence on the discharge temperature because the same oil quantity is injected at all oil inlet points. As the angle of the oil inlet point increases, the power efficiency decreases and so does the volumetric efficiency after passing through its maximum. Hence it should be possible to find an optimum position for the oil-injection port.

Oil droplet dynamics. The gas–oil heat transfer occurs during droplet free movement until the droplet reattaches to the wall of the compressor screws or housing. Following reference 20, the dominant external force governing the droplet is Stokes drag force defined by the coefficient

$$
\begin{aligned}
C_k &= \frac{4\mu Re C}{r^2 \rho} \\
C &= 24/Re \qquad Re < 0.3 \\
C &= 18.5/Re \qquad 0.3 < Re < 1000 \\
C &= 0.44 \qquad Re > 1000
\end{aligned} \tag{9}
$$

The resulting set of differential equations describing the movement of a droplet are:

$$
\begin{aligned}
\ddot{r} &= r\dot{\vartheta} - C_k\dot{r} \\
r\ddot{\vartheta} &= -2\dot{r}\dot{\vartheta} - C_k(r\dot{\vartheta} - \omega r) \\
\ddot{z} &= -C_k(\dot{z} - \omega r \mathrm{tg}\alpha)
\end{aligned} \tag{10}
$$

where dots denote the time derivatives.

The z-axis is coaxial with the axes of the compressor screws. Oil is injected through the nozzle in the compressor housing with velocity w. The initial conditions are

$$
\begin{aligned}
&\dot{r}(0) = w_r \qquad \dot{z}(0) = w_z \qquad \dot{\vartheta}(0) = w_{\vartheta}/r \\
&r(t_k) < r_e \qquad z(t_k) < -L
\end{aligned} \tag{11}
$$

All differential equations are solved by means of the Runge–Kutta fourth-order method. The calculation was made for a range of data by varying the droplet size, nozzle location and oil velocity, and finding the optimum values that produce the most efficient gas:oil heat transfer. *Figure 11* presents the calculated oil droplet trajectory for the highest gas–oil heat transfer efficiency, expressed in terms of axial and radial positions over the time period of droplet relative movement within the gas. The calculated values serve as input parameters for the oil nozzle design, expected to produce better oil atomization due to the considerable pressure drop in the nozzle and thus assuring an efficient oil injection.

It is obvious that for a larger compression chamber and for lower compressor shaft speeds the droplet active heat transfer time should be longer, which means that the problem of gas–oil transfer is emphasized for smaller compressors and for higher revolution speeds.

Optimum oil:gas ratio. Because the temperature variation in a screw compressor working chamber is strongly dependent on oil inlet temperature and oil:gas mass ratio, an analysis was made of oil temperature at the exit of the oil cooler. If the cooling capacity of the cooler is limited, the oil cooler outlet temperature is dependent on oil mass flow through the cooler. Although the processes of gas compression and oil cooling are both nonlinear, it is expected that the compression process is more dependent on oil inlet temperature, which means that the mini-

Table 2 Volumetric and power efficiency and specific power
Tableau 2 *Rendement volumétrique, puissance effective et puissance spécifique*

Droplet diameter (μm)	Oil inlet temperature (K)	Oil:gas mass ratio	Oil inlet position (deg)	Oil type (viscosity)	Volumetric efficiency	Power efficiency	Specific power (kW min m^{-3})
0	333	4	150	3	0.7065	0.6061	4.927
100	333	4	150	3	0.7056	0.6011	4.968
500	333	4	150	3	0.6960	0.5504	5.425
1000	333	4	150	3	0.6891	0.5067	5.894
0	293	4	150	3	0.7184	0.6797	4.393
0	313	4	150	3	0.7124	0.6411	4.658
0	333	4	150	3	0.7065	0.6061	4.927
0	353	4	150	3	0.7008	0.5745	5.198
0	373	4	150	3	0.6951	0.5456	5.473
0	333	0	150	3	0.6717	0.4021	7.427
0	333	2	150	3	0.7024	0.5812	5.138
0	333	4	150	3	0.7065	0.6061	4.927
0	333	6	150	3	0.7083	0.6165	4.844
0	333	8	150	3	0.7093	0.6222	4.799
0	333	4	0	3	0.7023	0.6108	4.889
0	333	4	90	3	0.7103	0.6156	4.851
0	333	4	150	3	0.7065	0.6061	4.927
0	333	4	210	3	0.6995	0.5831	5.121
0	333	4	270	3	0.6890	0.5362	5.569
0	333	4	150	1	0.6857	0.5895	5.066
0	333	4	150	2	0.6966	0.5982	4.992
0	333	4	150	3	0.7065	0.6061	4.927
0	333	4	150	4	0.7157	0.6135	4.868
0	333	4	150	5	0.7241	0.6202	4.815

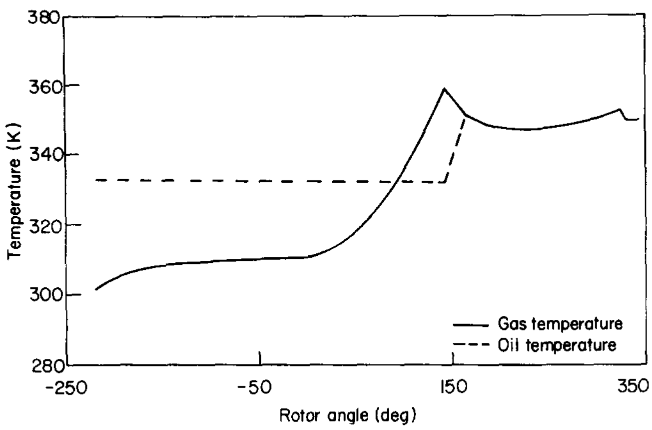

Figure 3 Predicted gas and oil temperature variation during the screw compressor cycle with Sauter mean oil droplet size $d = 0$ μm
Figure 3 *Variation prévue de la température du fluide et de l'huile, au cours du cycle du compresseur à vis, avec la dimension moyenne de la gouttelette d'huile de Sauter d = 0 μm*

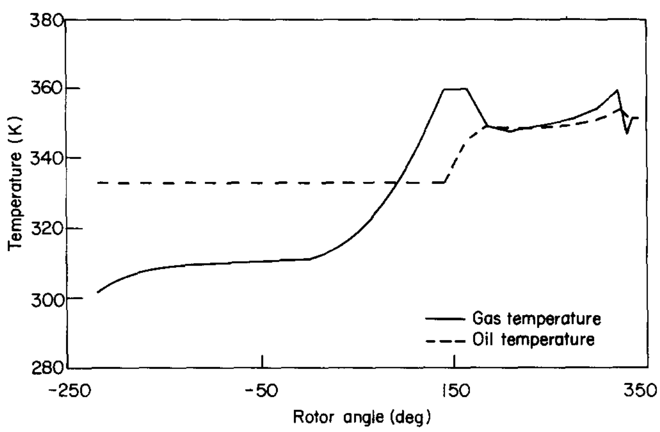

Figure 4 Predicted gas and oil temperature variation during the screw compressor cycle with Sauter mean oil droplet size $d = 100$ μm
Figure 4 *Variation prévue de la température du fluide et de l'huile, au cours du cycle du compresseur à vis, avec la dimension moyenne de la gouttelette d'huile de Sauter d = 100 μm*

mum oil temperature at the compressor outlet (oil cooler inlet) could not be found. Hence for the purpose of mathematical modelling of screw compressor plant the oil mass variation was employed as an optimization parameter. The results are presented in *Table 3* and in a diagram in *Figure 12* (the same compressor as in *Table 2*, both for a delivery pressure of 9 bar).

It can be seen from *Table 2* that there is an optimum value of oil mass flowrate resulting in the minimum compressor outlet oil temperature, which corresponds closely to the minimum compressor specific power. The optimum value of compressor oil flow was also confirmed experimentally to yield a basis for the compressor plant design and plant components construction.

Laboratory experimental investigation

Test rig and measuring equipment

The cyclic gas compression in a screw compressor imposes a non-stationary pulsating fluid motion, so measurement of the instantaneous values of individual characteristics requires instruments of high dynamic response and with a large frequency range. At the same time, owing to the restricted space for their mounting, the transducers must have small overall dimensions, so that their presence does not spoil the physical and geometrical conditions of the compressor operation[7]. The following bulk operating characteristics were measured: delivery rate, power consumption, power utilization

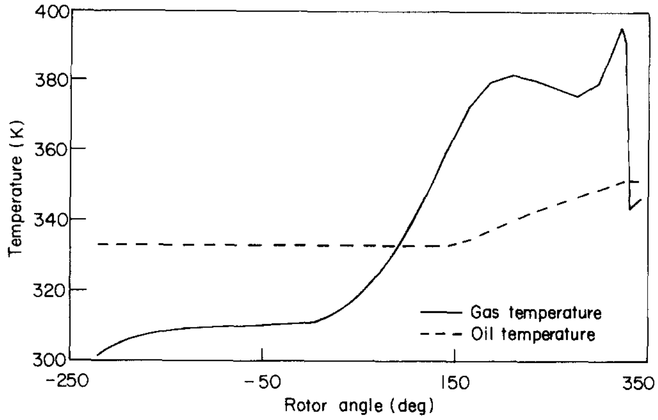

Figure 5 Predicted gas and oil temperature variation during the screw compressor cycle with Sauter mean oil droplet size d = 500 µm
Figure 5 *Variation prévue de la température du fluide et de l'huile au cours du cycle du compresseur à vis, avec la dimension moyenne de la gouttelette d'huile de Sauter d = 500 µm*

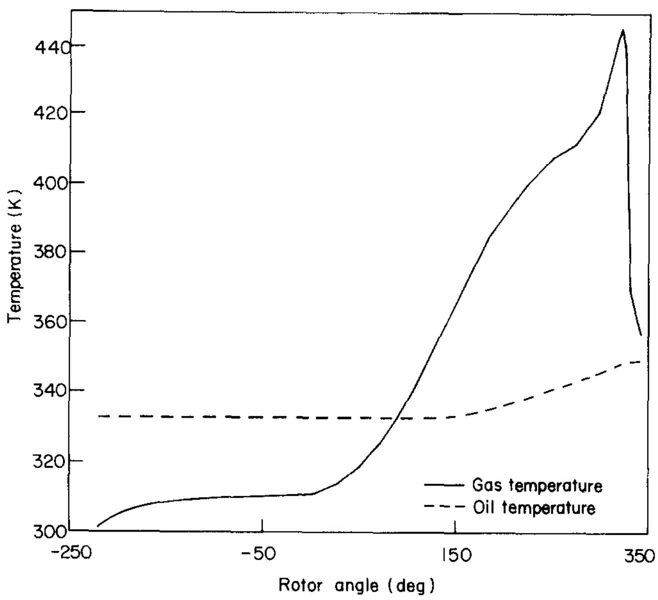

Figure 6 Predicted gas and oil temperature variation during the screw compressor cycle with Sauter mean oil droplet size d = 1000 µm
Figure 6 *Variation prévue de la température du fluide et de l'huile au cours du cycle du compresseur à vis, avec la dimension moyenne de la gouttelette d'huile de Sauter d = 1000 µm*

efficiency, specific power, gas and oil temperatures. In addition, the instantaneous values of all relevant pulsating quantities were also recorded for the purpose of studying the details of the thermodynamic cycle, in particular the pressure in the compressor swept volume as the basis for devising the p–V diagram. For this purpose a new method was developed for constructing the compressor indicator diagram, which employs the recordings of the pressure changes at several discrete points along the fluid path over a period of time (range of rotating angle[12]).

A sketch of the measuring installation is presented in *Figure 13*, which illustrates the main components of the compressor set, positions of the transducers and their coupling with the data acquisition and processing system. As can be seen, the compressed gas, contami-

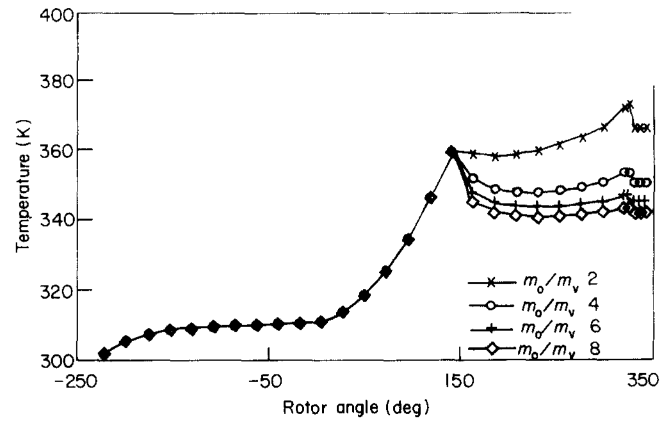

Figure 7 Predicted influence of oil:gas mass ratio on air temperature during the compressor cycle
Figure 7 *Influence prévue du rapport massique huile/fluide sur la température du fluide, au cours du cycle du compresseur*

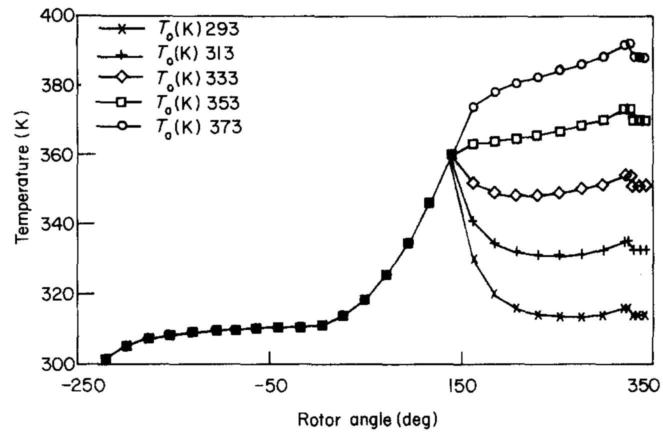

Figure 8 Predicted influence of oil inlet temperature on gas temperature during the compressor cycle
Figure 8 *Influence prévue de la température d'aspiration de l'huile sur la température du fluide au cours du cycle du compresseur*

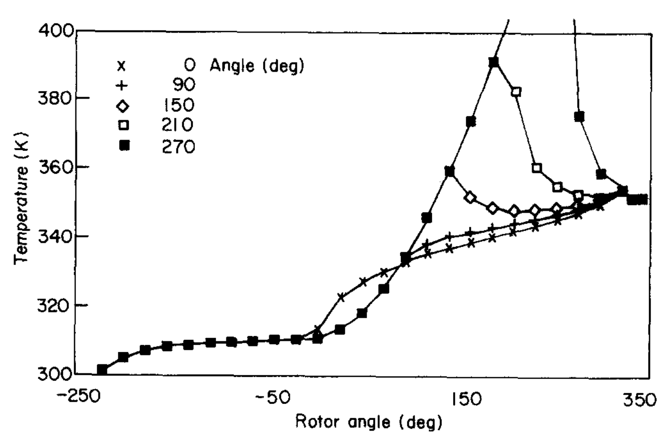

Figure 9 Predicted influence of oil injection position on gas temperature during the compressor cycle
Figure 9 *Influence prévue de la localisation de l'injection d'huile sur la température du fluide au cours du cycle du compresseur*

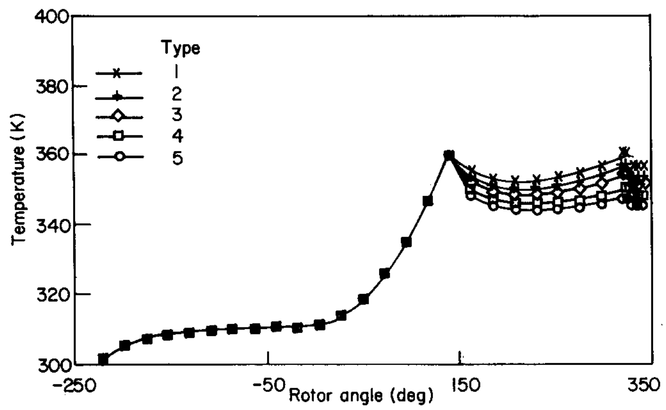

Figure 10 Predicted influence of oil type (viscosity) on gas temperature during the compressor cycle
Figure 10 *Influence prévue du type d'huile (viscosité) sur la température du fluide au cours du cycle du compresseur*

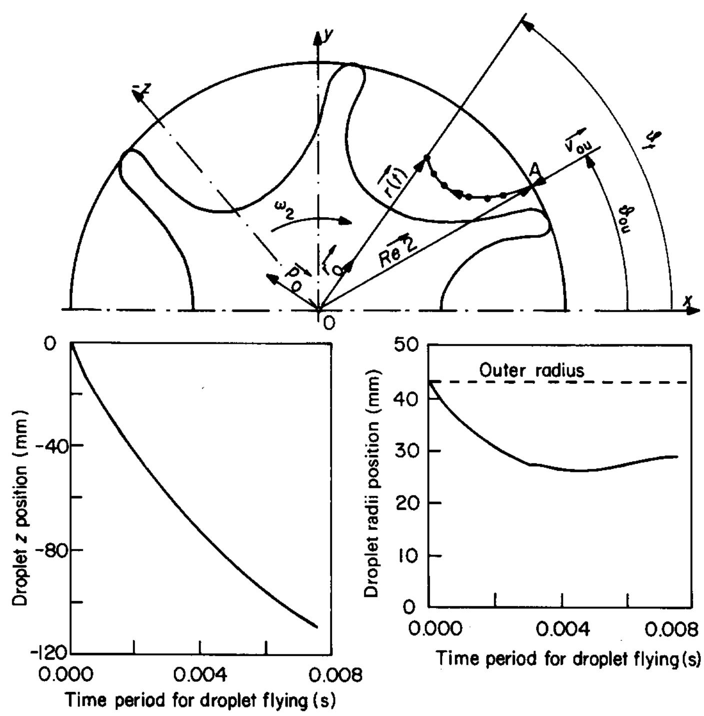

Figure 11 Oil droplet trajectories in the gate screw domain
Figure 11 *Trajectoires de la gouttelette d'huile dans la région de la porte du compresseur à vis*

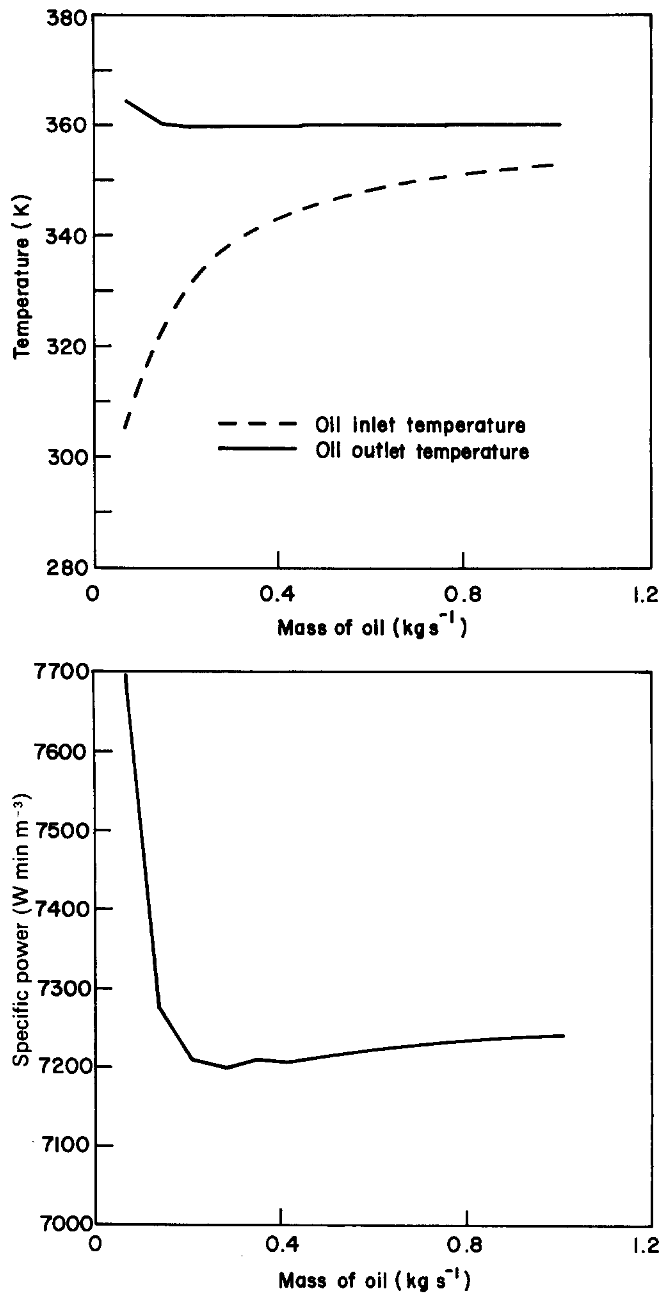

Figure 12 Predicted oil:mass ratio influence on the compressor plant overall performances
Figure 12 *Influence prévue du rapport massique de l'huile sur les performances globales du compresseur*

Table 3 Determination of oil injection mass flowrate
Tableau 3 *Détermination de débit masse de l'huile injectée*

M_o (kg s^{-1})	t (K)	t (K)	N_s (W min m^{-3})	M_o (kg s^{-1})	t (K)	t (K)	N_s (W min m^{-3})
0.069	305.1	364.6	7698	0.595	348.2	359.8	7221
0.140	322.2	360.4	7275	0.665	349.4	359.9	7226
0.210	331.5	359.7	7209	0.735	350.4	359.9	7231
0.280	337.2	359.6	7199	0.805	351.2	360.0	7234
0.350	341.1	359.6	7210	0.875	351.9	360.0	7237
0.420	343.8	359.7	7207	0.945	352.4	360.1	7240
0.490	345.9	359.8	7214	1.014	353.0	360.1	7242

nated by the oil, enters first the oil separator and, after being decontaminated, is ducted into the gas reservoir. The oil separated from the gas in the oil separator is taken into the oil cooler and then injected back into the compressor. The compressor investigated was driven by a 75 kW 2490 rev. min^{-1} electrical motor coupled with a compressor via a torque transmission gear which ensured the compressor rotation speed was increased by a ratio of 1.723. At the end of the shaft, a torque transducer was mounted together with an optical revolution indicator, connected to an amplifier and electronic counter.

Suction and discharge parameters were measured by placing the pressure and temperature sensors at the compressor inlet after the suction gas filter and at the engine exit port, respectively. A vortex flowmeter for measuring the gas flowrate was installed at the outlet of the oil

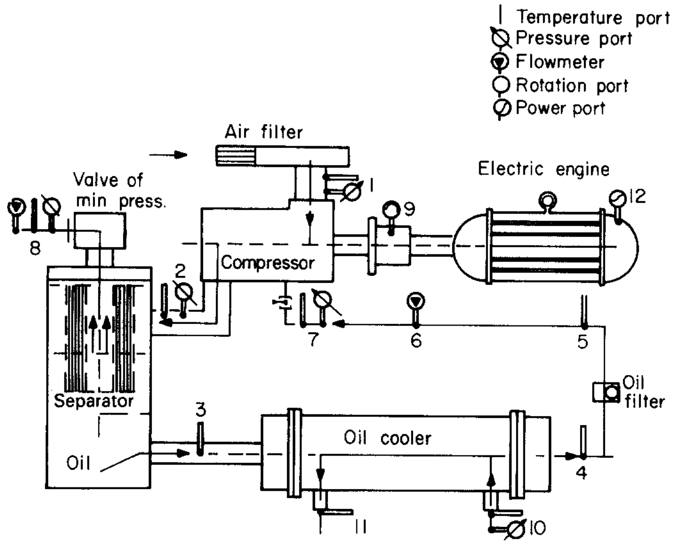

Figure 13 The test installation: 1, compressor inlet, gas; 2, compressor outlet, gas; 3, oil cooler inlet, oil; 4, oil cooler outlet, oil; 5, 6, 7, compressor inlet, oil; 8, oil separator outlet, gas; 9, torque shaft and speed of revolution; 10, oil cooler inlet, cooling water; 11, oil cooler outlet, cooling water
Figure 13 *Installation expérimentale: 1, aspiration au compresseur, fluide; 2, refoulement au compresseur, fluide; 3, entrée du refroidisseur d'huile, huile; 4, sortie du refroidisseur d'huile, huile; 5,6,7, aspiration du compresseur, huile; 8, sortie du séparateur d'huile, fluide; 9, couple et vitesse de rotation; 10 entrée du refroidisseur d'huile (eau de refroidissement); 11, sortie du refroidisseur d'huile (eau de refroidissement)*

separator just in front of the gas reservoir. Oil temperature at the compressor inlet, as well as at the oil cooler inlet and outlet, and the oil flowrate were also measured. A general view of a compressor test rig is given in *Figure 14*.

The working volume of a screw compressor has a complex shape passing through the compressor along the axial and tangential direction. For this reason several pressure transducers had to be installed into the screw compressor casing and used simultaneously for recording the experimental data. Four holes were drilled in the casing along the direction parallel to the longitudinal screw axis (while the main and the gate screws were removed) to accommodate the transducers. A specially designed adaptor was used for installing the pressure gauge at the selected measuring point. The electrical signal from the transducer was brought through the coaxial cable to the corresponding converter and amplifier and then to the cathode oscilloscope with memory, on which the pressure variations with time were monitored. On the basis of known overall compressor geometry, the working volume and its change with time/rotation angle, the arrangement of the measuring points on the compressor housing and recordings of the instantaneous pressure at several points in the working space, it was possible to obtain the p–α and p–V diagrams. Typical recordings of three pressure transducers are presented in *Figure 15*, while the plots of p–α and indicating diagrams are presented in *Figures 16–21*.

As can be seen from pressure recordings in *Figure 15*, each of the three pressure gauges covers an angle range of about 80°. By adopting the zero value of the rotating angle of the main rotor to be at the beginning of the compression, the ranges of the angles of rotation covered by individual pressure gauges were: first gauge, 133.2–213.4°; second gauge, 211.4–291.6° (both covering the major portion of the compression process); and third gauge, 289.5–360.7° (covering the last stage of the compression and the exhaust period). It should be noted that the exhaust process starts at the angle of 292°. The oil injection into the compression chamber begins at the angle of 168° and lasts through the next 79.5° of rotation of the main rotor. Pressure value is obtained by multiplying by mesh size.

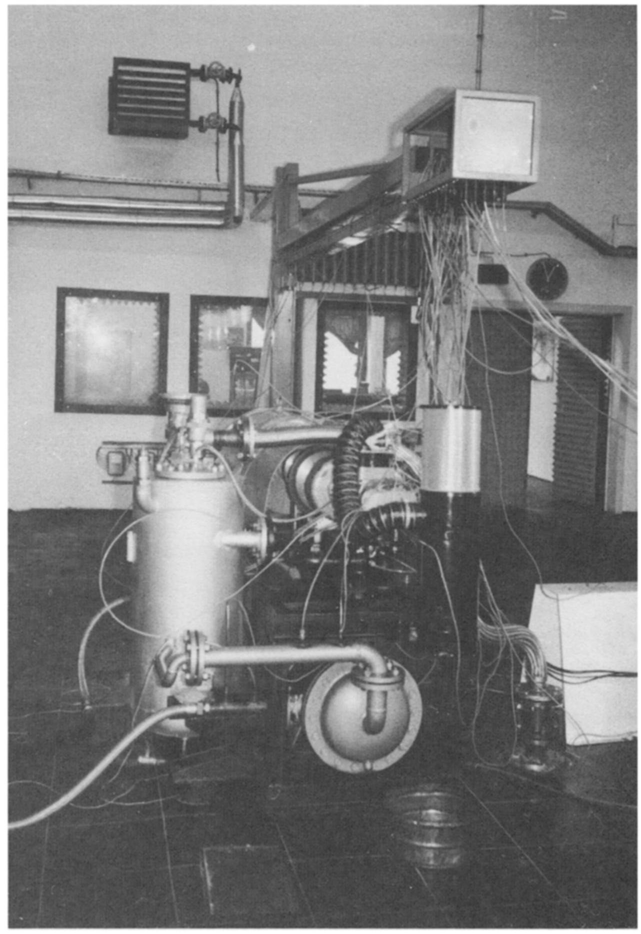

Figure 14 A general view of the compressor testing rig
Figure 14 *Vue générale du banc d'essai du compresseur*

Recording and acquisition of the measured data were achieved with an AVL Test Commander Compressor Tester. The equipment consists of a Motorola microprocessor MC 6800 with ACIA interface module, VDU control module and floppy control module, analogue–digital converters, four six-channel multiplexers MUX (0–10 V (d.c.) and 0–20 mA (d.c.)), and separate sets for measuring temperature, pressure, torque and electric power consumption. *Table 4* outlines the basic characteristics of the data measuring and acquisition system.

Discussion

The results obtained by experimental investigations and mathematical modelling of the influence of oil injection on the screw compressor working process will be discussed in two different contexts: first, comparison of the experimental and mathematically modelled and computed p–α and p–V diagrams and, secondly, analysis and discussion of the overall parameters (in *Tables 5* and *6*).

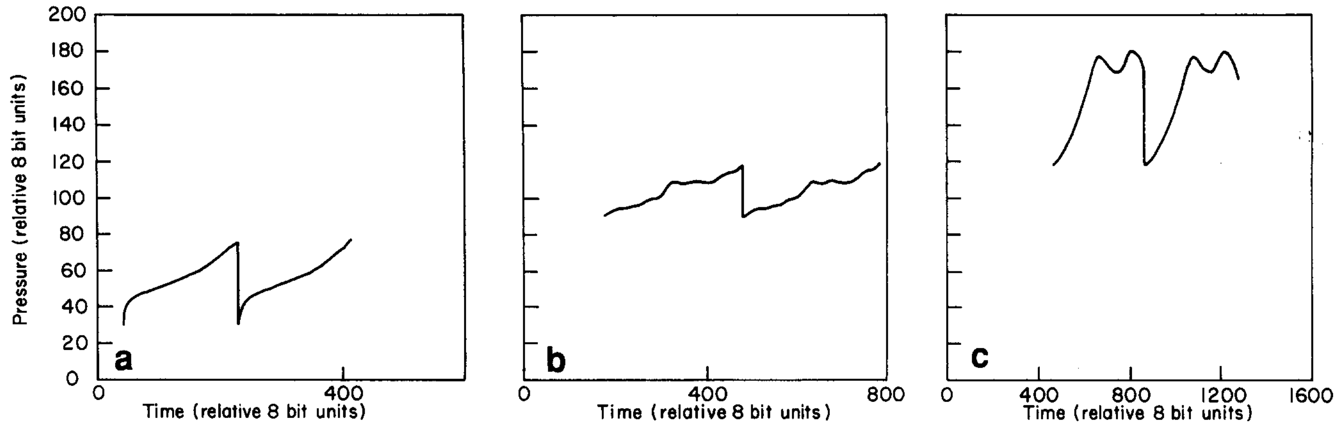

Figure 15 Pressure transducer records in the screw compressor chamber: (a) transducer 1, compression (133–213°); (b) transducer 2, compression (211–292°C); (c) transducer 3, compression and outflow (290–361°)
Figure 15 *Enregistrements du transducteur de pression dans la chambre du compresseur à vis: (a) transducteur 1, compression (133–213°); (b) transducteur 2, compression (211–292°); (c) transducteur 3, compression et écoulement (290–361°)*

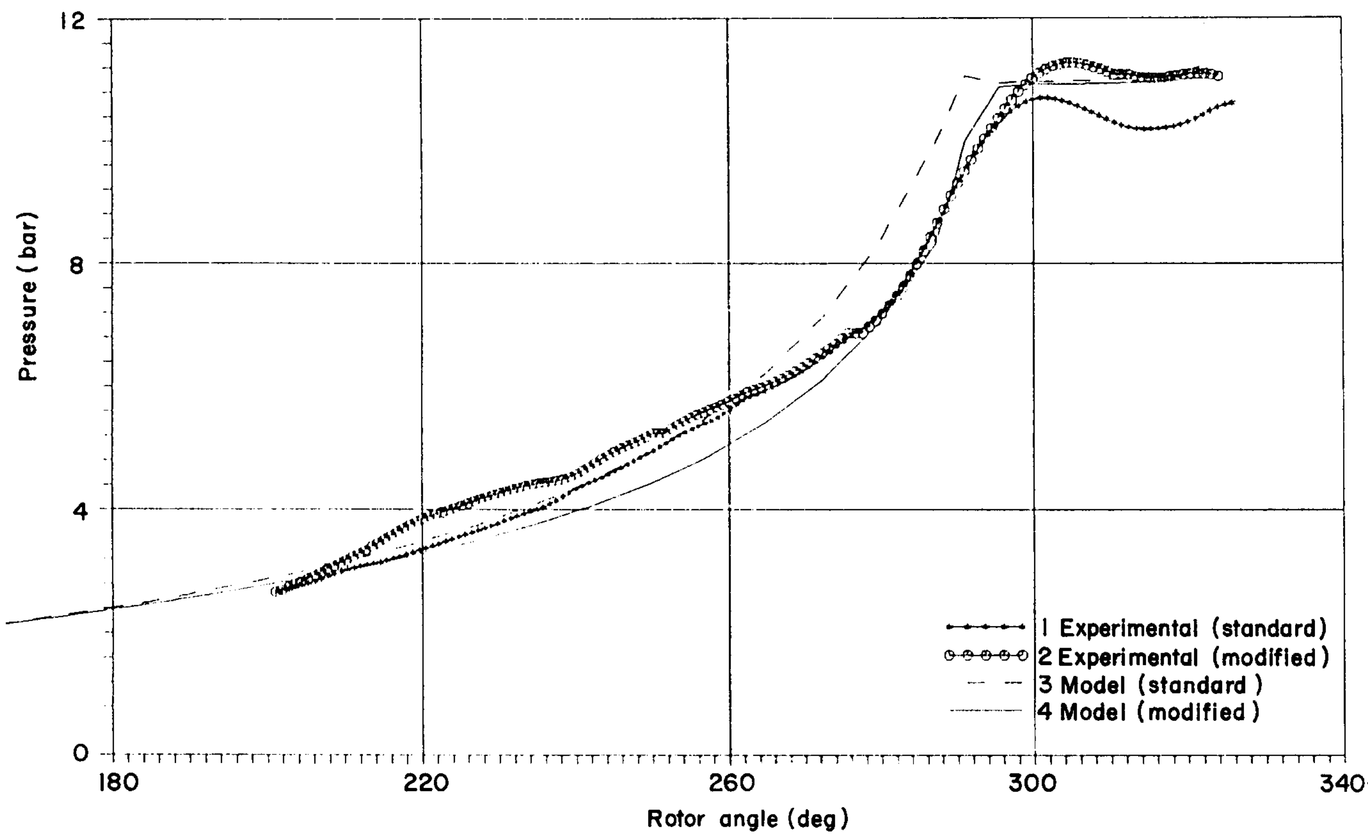

Figure 16 p–α diagram (outlet pressure 9 bar)
Figure 16 *Diagramme p–α (pression de refoulement 9 bars)*

In *Figures 16* and *17* diagrams of the pressure in the compression chamber are plotted over the rotation angle of the main rotor and over the compressor swept volume, presenting the p–α and p–V diagrams for compressor outlet pressure of 9 bar. *Figures 18–21* show two other sets of plots of the same variables, but for compressor outlet pressures of 11 and 13 bar, respectively. Two different oil injection systems were considered: the standard system, which has already been in use in 'Trudbenik' screw compressors, and a modified system with a newly designed oil nozzle. For the latter, the nozzle was placed at the position and oriented in the direction that (in accord with both the experimental findings and computer simulation) were supposed to yield the best gas–oil heat transfer performances. All figures contain four curves, two for each oil-injection system considered. Curves denoted by 1 and 2 refer to the standard and 3 and 4 denote the modified system. The experimental data are denoted by dots, while the results obtained by the model computations are presented by lines. All of the results indicate that the pressure records obtained by a modified oil-injection system gave a lower pressure gradient during compression than results recorded with the standard oil-injection system. This phenomenon can be explained by a better gas–oil heat transfer during the first stages of oil injection, which considerably reduces

Table 4 Measuring equipment used in the experimental investigation
Tableau 4 *Equipements de mesure utilisés dans la recherche expérimentale*

Measuring value	Measuring equipment	Characteristics
Static pressure	Pressure transducer AVC200	range 120 mbar–20 bar output 0–20 mA accuracy 0.3%
Dynamic pressure	Piezoelectric pressure transducer XTME-190M Amplifier D81	range 0–17 bar 3.54 mV bar^{-1} output 0–10 V accuracy 0.1%
Temperature	Thermocouple NiCr–Ni Reference thermostat VST6 Measuring d.c. differential amplifier	range − 10–250°C output 0–10 V accuracy 0.1%
Shaft torque and speed of revolution	Torque shaft T30FN3/2	range 0–2 kNm 0–7000 rev. min^{-1} accuracy 0.2%
	Torque transducer MD3555	range 0–5 kNm 0–7000 rev. min^{-1} output 0–10 V (d.c.) accuracy 2%
	RPM transducer N3556C	range 0–5000 rev. min^{-1} output 0–10 V (d.c.) accuracy 0.1%
Compressor delivery	Vortex flowmeter SWZ50Ag71.1/F2	range 0–4 m^3 min^{-1} 2.5–30 bar accuracy 1%
	Signal transducer SAW1.1UR10–S20Z	range 0–20 mA (d.c.) accuracy 0.1%
Oil flow	Rotameter OI50Ag19E/G1	range 0–250 l min^{-1} 0–25 bar accuracy 2%
	Impulse amplifier with current output ZIVVS20W	range 0–20 mA (d.c.)

Table 5 Experimental results for different outlet pressures corrected for oil flow and shaft revolution speed
Tableau 5 *Résultats expérimentaux pour différentes pressions de refoulement, en fonction du débit d'huile et de la vitesse de rotation de l'arbre*

		Oil system 1			
Outlet pressure	bar	9.00	11.00	13.00	15.00
Compressor delivery	m^3 min^{-1}	3.68	3.63	3.40	3.30
Shaft revolution speed	rev min^{-1}	5161	5161	5161	5161
Specific power	kW min m^{-3}	7.12	7.97	8.75	9.59
Compressor power	kW	27.20	28.94	29.72	31.65
Oil flow	l min^{-1}	43.28	45.60	50.74	53.66
Oil inlet temperature	K	329.6	322.4	332.6	333.9
Gas/oil outlet temperature	K	346.8	342.9	340.8	340.7
Delivery efficiency	—	0.785	0.78	0.72	0.70
Power efficiency	—	0.523	0.50	0.49	0.47
		Oil system 2			
Outlet pressure	bar	9.00	11.00	13.00	15.00
Compressor delivery	m^3 min^{-1}	3.56	3.65	3.42	3.32
Shaft revolution speed	rev min^{-1}	5161	5161	5161	5161
Specific power	kW min m^{-3}	6.84	7.56	8.44	9.33
Compressor power	kW	25.31	27.65	28.85	30.98
Oil flow	l min^{-1}	43.28	45.60	50.74	53.66
Oil inlet temperature	K	332.4	332.4	332.6	333.9
Gas/oil outlet temperature	K	343.6	342.7	341.8	341.7
Delivery efficiency	—	0.759	0.78	0.73	0.71
Power efficiency	—	0.572	0.53	0.51	0.51

Table 6 A comparison of experimental and modelled results
Tableau 6 *Comparaison des résultats expérimentaux et de modélisation*

		Oil system 1		Oil system 2	
		Model	Exp.	Model	Exp.
Outlet pressure	bar	9.00	9.00	9.00	9.00
Compressor delivery	m^3 min^{-1}	3.63	3.68	3.66	3.56
Shaft revolution speed	rev. min^{-1}	5151.82	5161.00	5151.82	5163.00
Teeth tip velocity	m s^{-1}	28.90	28.90	28.90	28.90
Specific power	kW min m^{-3}	7.30	7.12	6.76	6.84
Compressor power	kW	26.53	27.20	24.76	25.31
Oil flow	l min^{-1}	39.40	43.28	39.40	38.64
Oil inlet temperature	K	323.80	329.60	323.80	323.80
Gas/oil outlet temperature	K	340.60	346.80	336.80	343.60
Gas temperature after compression	K	388.00	—	357.40	—
Delivery efficiency	—	0.78	0.785	0.78	0.759
Power efficiency	—	0.50	0.523	0.54	0.572

the temperature rise of gas during the compression, retaining a lower index of the polytrope. Lower values of the compressor indicator and effective power should be expected in this case, ensuring a better power consumption efficiency and an even better compressor delivery efficiency. This phenomenon is especially evident for lower delivery pressure (9 and 11 bar), and its influence becomes less important at higher outlet pressures (*Table 5*).

A set of overall results is presented in *Table 6* showing a comparison of model calculations with experimental data for the outlet pressure of 9 bar. It should be emphasized that the highest gas temperature (this occurs at the end of compression before the gas–oil heat transfer is completed), obtained directly by modelling and calculated indirectly from experimental data by the heat balance of the compressor gave up to 30°C lower values with the modified oil-injection system than for the standard one. This temperature difference is assumed to originate as a consequence of two effects. First, the more efficient oil injection in the modified system results in better gas cooling and consequently a more moderate gas temperature rise than the standard injection system. Secondly, the pressure slope obtained by the modified system better fits the built-in compression ratio, thereby avoiding the external expansion (noticed in the standard system), which is more evident for the lower delivery pressures.

The results of the experimental investigation are compared with the results of mathematical modelling for experimental conditions (*Figures 16–21* and *Table 6*). The comparison confirms that the mathematical model adequately describes the process modelled. All results proved the positive effects of the reconstruction of oil-injection system:

1. The oil mass ratio was reduced by 2–3% as compared with the previous oil systems;
2. The same compressor delivery was achieved with a power consumption reduced by 2.76–7.42%;
3. Since the pressure increase itself promotes better oil

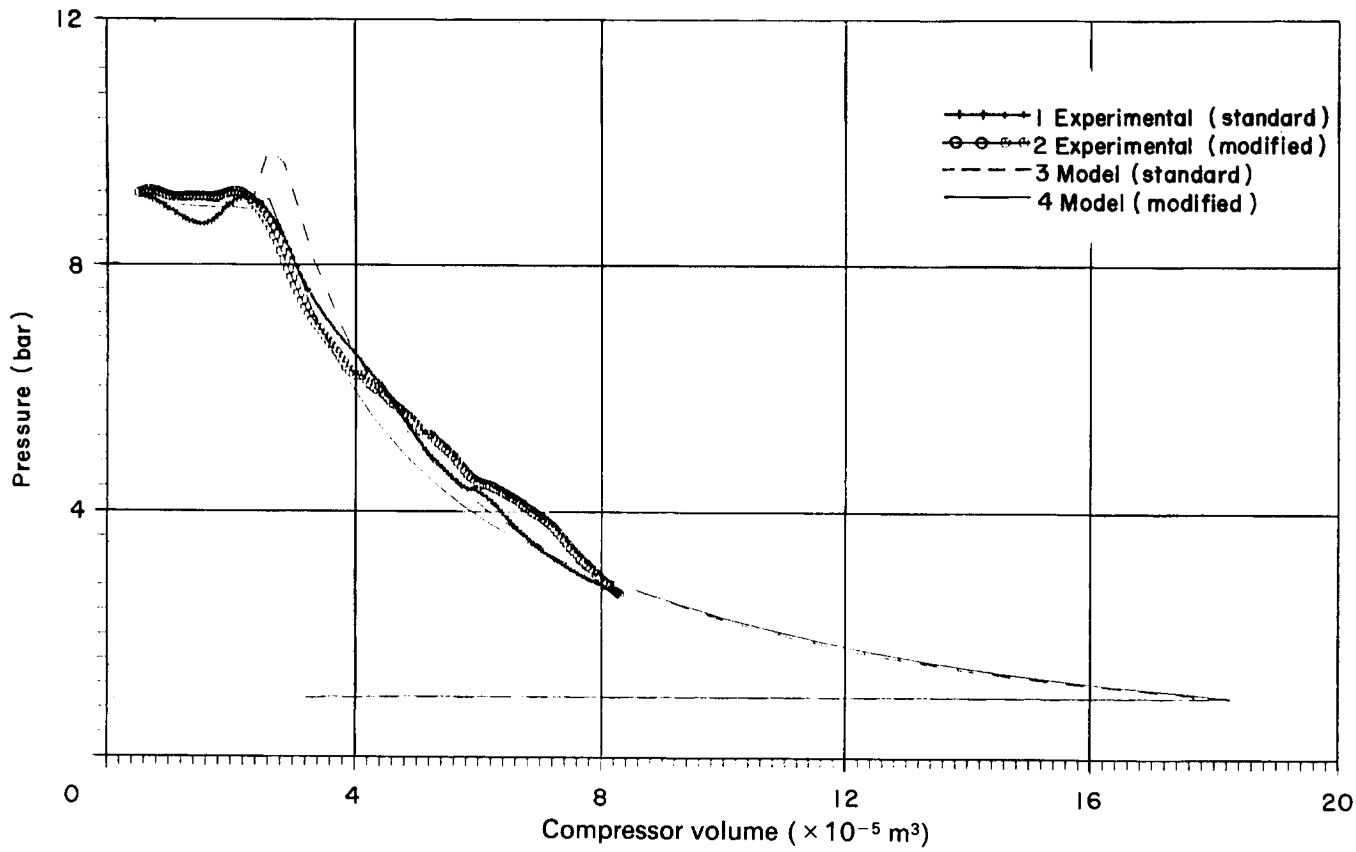

Figure 17 p–V diagram (outlet pressure 9 bar)
Figure 17 *Diagramme p–V (pression de refoulement 9 bars)*

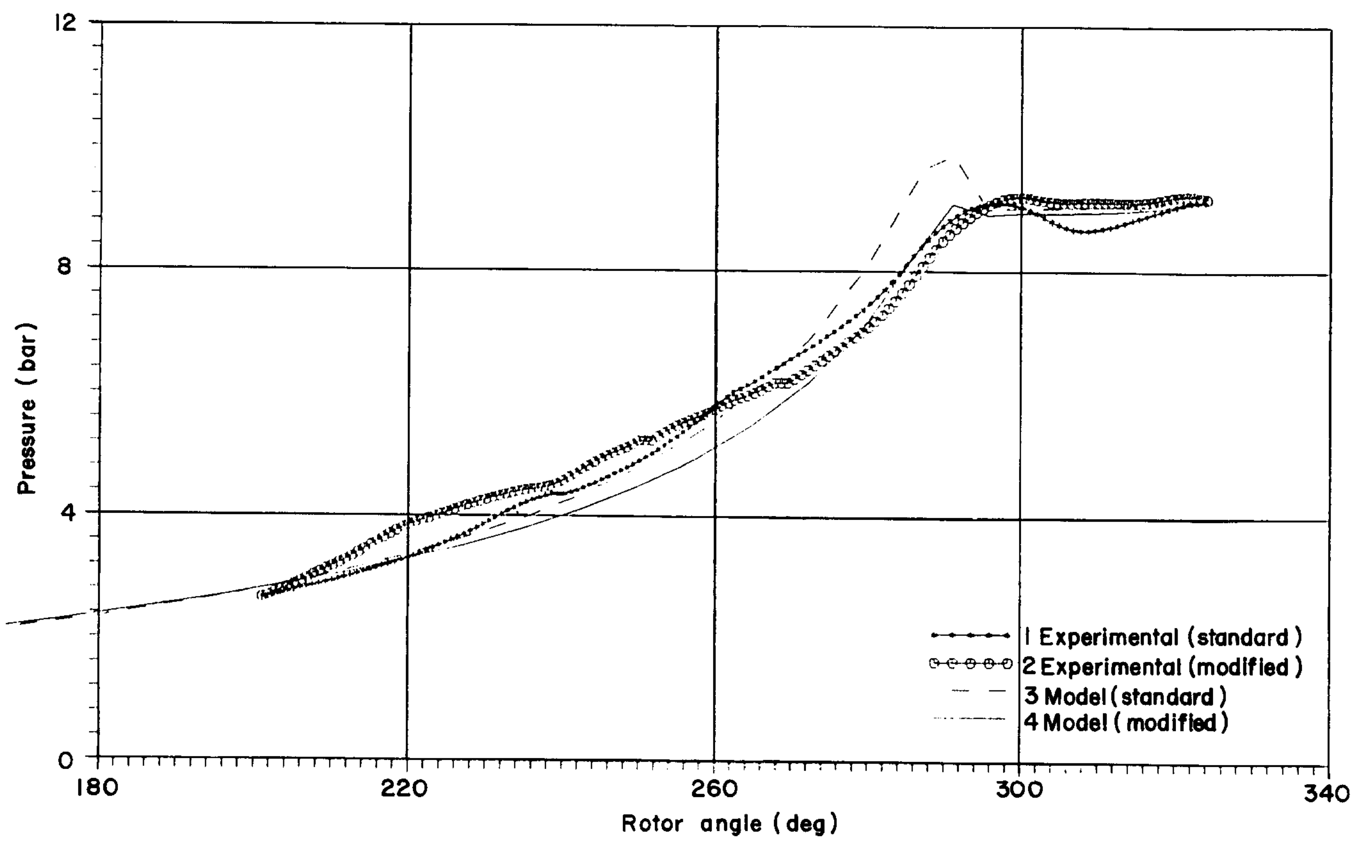

Figure 18 p–α diagram (outlet pressure 11 bar)
Figure 18 *Diagramme p–α (pression de refoulement 11 bars)*

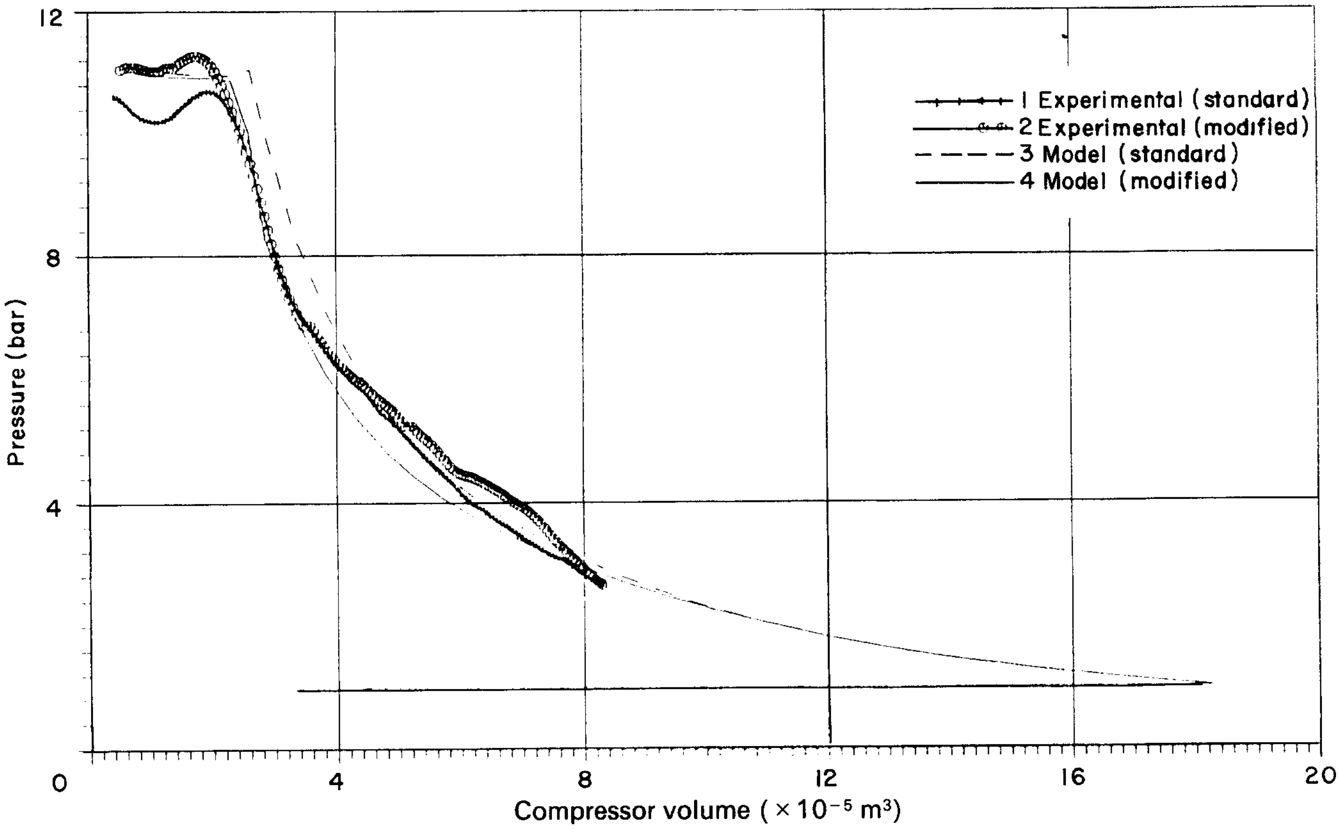

Figure 19 *p–V* diagram (outlet pressure 11 bar)
Figure 19 *Diagramme p–V (pression de refoulement 11 bars)*

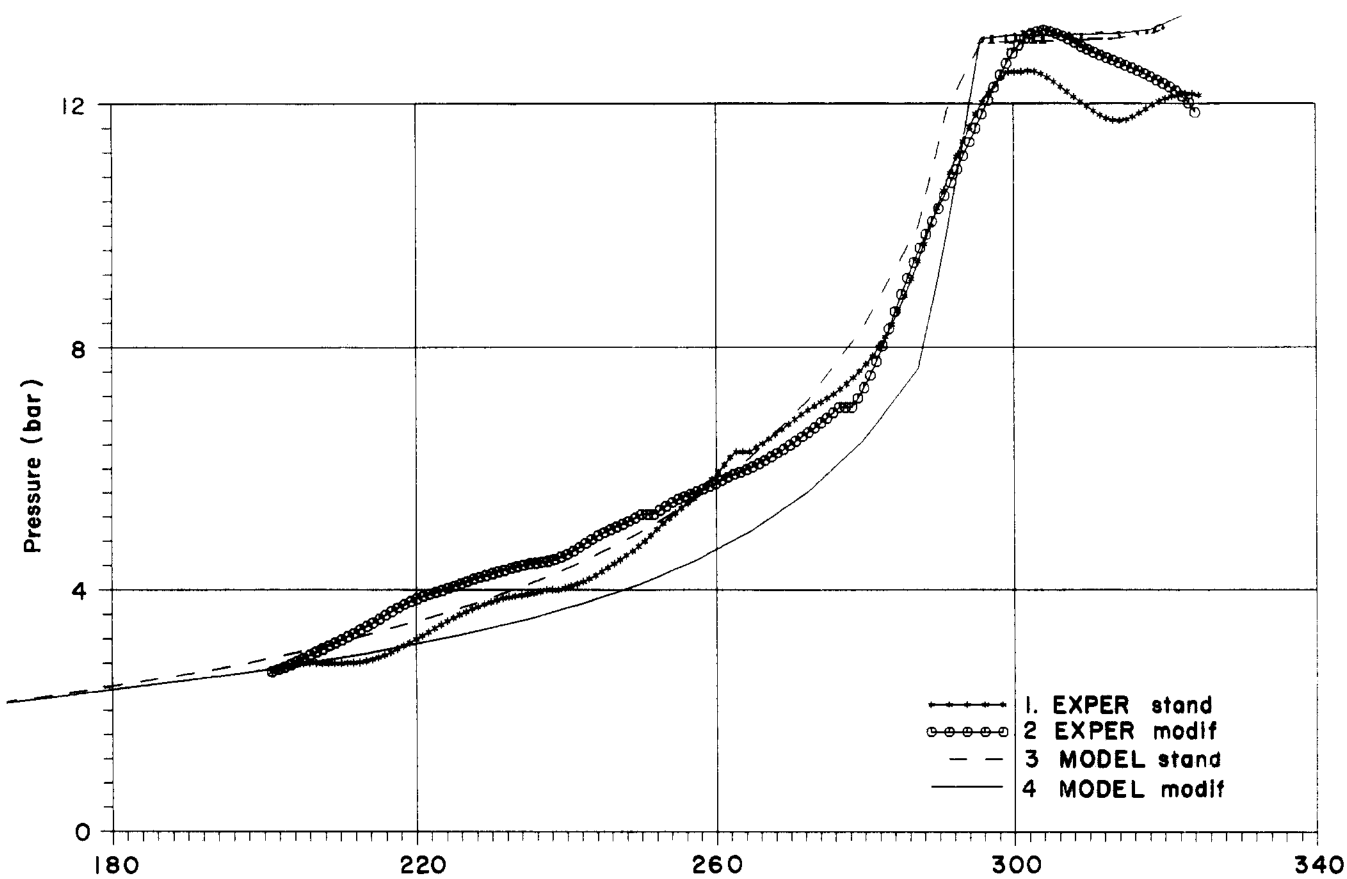

Figure 20 *p–α* diagram (outlet pressure 13 bar)
Figure 20 *Diagramme p–α (pression de refoulement 13 bars)*

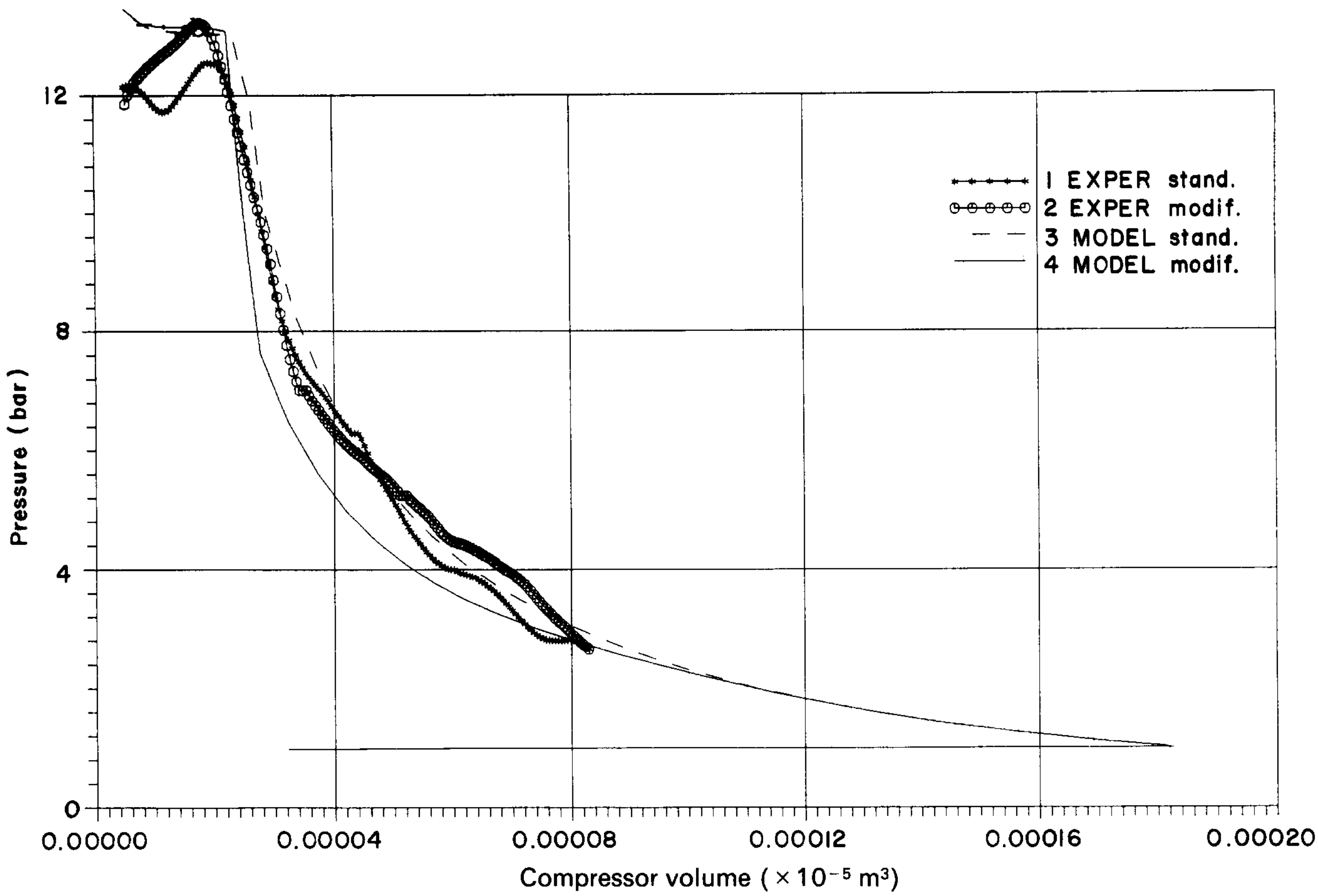

Figure 21 *p–V* diagram (outlet pressure 13 bar)
Figure 21 *Diagramme p–V (pression de refoulement 13 bars)*

atomization, this improvement fades out with an increase of delivery pressure, reducing the benefits of the reconstruction.

Conclusions

After a comprehensive analysis of the influence of various parameters of an oil-injection system upon a screw-compressor working cycle, made experimentally and by means of a computer simulation, a new modified system with a more efficient nozzle was designed for Energoinvest-Trudbenik screw compressors.

It can be concluded that the temperature of the oil follows the gas temperature during the compressor cycle closely, except for extremely large oil droplet sizes (over 0.5 mm). An important influence of the oil temperature and oil injection location has been noticed, but the oil:gas mass ratio and the oil viscosity have a surprisingly small influence on the compressor process.

Experimental investigations of two prototypes of screw compressor (one of them equipped with the standard and another with the new modified oil-injection system) enabled a detailed insight into the effects of all relevant parameters upon the screw compressor performances. In comparison with previous solutions, the new oil system proved to be more efficient and resulted in lower oil consumption, better gas cooling and an improvement in overall compressor performances. Both the model and the experiments lead to a conclusion that a considerable decrease of compressor specific power consumption and oil-injection mass flow ratio could be achieved by a change of the nozzle diameter and its position. The savings achieved are higher for smaller compressors and for lower and moderate-pressure ratios. The experiments also confirmed the validity of the basic concept of the mathematical model and its applicability to the CAD[24] of compressor systems.

Acknowledgement

The investigations reported in this paper were made within the framework of the research project on Development of Mathematical Models of Screw Compressors as a Basis for the Computer Aided Design sponsored by Science Foundation of Republic of Bosnia and Hercegovina, Yugoslavia. The experimental investigations were made at Energoinvest Trudbenik Compressor Laboratories in Doboj, Yugoslavia.

References

1 **Aburaya, S.** A study of simulation model for rotary compressors *J Soc Mech Engrs* (1980)
2 **Amosov, P. E. *et al.*** *Vintovie kompresprnie mashinii – spravochnik* Mashinstroienie Leningrad (1977)
3 **Bein, T. W., Hamilton, J. F.** Computer modeling of an oil flooded single screw air compressor *Proc Purdue Compressor Technol Conf* (1982) 127
4 **Blaise, J. C., Dutto, T.** Influence of oil injection and pressure ratio on single screw performances at high temperature *Proc Int Compressor Engng Conf at Purdue* (1988)
5 **Brablik, J.** Analytical model of an oil-free screw compressor *Proc Purdue Compressor Technol Conf* (1982) 356

6 **Chan, C. Y., Haselden, G. G.** Computer simulation of oil-free operation of the single screw compressor *Proc IIR* (1984) 48
7 **Deblois, R., Stoeffler, R. C.** Instrumentation and data analysis techniques for scroll compressor *Proc Int Compressor Engng Conf at Purdue* (1988)
8 **Firnhaber, M. A., Szarkowicz, D. S.** Modeling and simulation of rotary screw compressors *Proc Purdue Compressor Technol Conf* (1980) 305
9 **Fujiwara, M., Kasuya, K.** Computer modeling for performance analysis of rotary screw compressor *Proc Purdue Compressor Technol Conf* (1984) 536
10 **Hamilton, J. F.** *Extensions of Mathematical Modeling of Positive Displacement Type Compressors* Ray W. Herrick Laboratories, Purdue University (1974)
11 **Hanjalić, K., Stošić, N.** Some aspects of laboratory testing of two-stage reciprocating compressors *Proc 4th Purdue Compressor Technol Conf, Lafayette, USA* (1978)
12 **Hanjalić, K., Stošić, N., Arslanagić, M.** Contribution towards a development of measuring methods for complex investigations of displacement compressors *Tehnika J* (October 1980) (in Serbo-Croat)
13 **Kovačević, A., Stošić, N.** Measuring and data acquisition of screw compressor working process parameters *Proc 20th JUR-EMA Smp, Zagreb* (April 1988) (in Serbo-Croat)
14 **Maclaren, J. F. T.** The influence of computers on compressor technology *Proc Purdue Compressor Technol Conf* (1982) 1
15 **Ng, E. H, Tramschek, A. B., Maclaren, J. F. T.** Computer simulation of a reciprocating compressor using a real gas equation of state *Proc Purdue Compressor Technol Conf* (1980) 33
16 **Rinder, L.** *Scraubenverdichter* Springer Verlag, New York (1979)
17 **Sakun, I. A.** *Vintovie kompresorii*, Mashinostroenie Leningrad (1970)
18 **Sangfors, B.** Analytical modeling of helical screw machine for analysis and performance prediction *Proc Purdue Compressor Technol Conf* (1982)
19 **Sangfors, B.** Computer simulation of the oil injected twin screw compressor *Proc Purdue Compressor Technol Conf* (1984) 528
20 **Singh, P. J., Patel, G. C.** Generalized performance analysis of oil flooded twin-screw compressors *Proc Purdue Compressor Technol Conf* (1984) 544
21 **Singhal, J. P., Prakash, R., Varma, H. K.** Simulation for thermodynamic aspects of reciprocating refrigerant compressors using real gas properties *Proc Purdue Compressor Technol Conf* (1982) 239
22 **Soedel, W.** *Introduction to Computer Simulation of Positive Displacement Compressors* R. Herrick Laboratories, Purdue University (1972)
23 **Stošić, N., Kovačević, A., Hanjalić, K., Milutinović, Lj.** Mathematical modelling of the oil influence upon the working cycle of screw compressors *Proc 14th Int Compressor Engng Conf at Purdue, Lafayette, USA* (July 1988)
24 **Stošić, N., Hanjalić, K.** Development and optimization of a new family of screw compressors by computer modelling, *Proc Int Forum on Mathematical Modelling and Computer Simulation in Energy Systems, Sarajevo* (1989)
25 **Stošić, N., Hanjalić, K., Ivanović, M., Koprivica, J., Lovren, N.** Computer aided design of screw compressor elements *Strojarstvo J* (1986) **28** 3 (in Serbo-Croat)
26 **Stošić, N., Hanjalić, K., Koprivica, J.** A contribution towards the mathematical modelling of screw compressor working process *Strojarstvo J* (1986) **28** 95 (in Serbo-Croat)